Caveolin-1 Ablation Reduces the Adverse Cardiovascular Effects of *N*-ω-Nitro-L-Arginine Methyl Ester and Angiotensin II

Luminita H. Pojoga, Jose R. Romero, Tham M. Yao, Paul Loutraris, Vincent Ricchiuti, Patricia Coutinho, Christine Guo, Nathalie Lapointe, James R. Stone, Gail K. Adler, and Gordon H. Williams

Department of Endocrinology, Diabetes, and Hypertension (L.H.P., J.R.R., T.M.Y., P.L., V.R., P.C., C.G., N.L., G.K.A., G.H.W.), Brigham and Women's Hospital/Harvard Medical School, Boston, Massachusetts 02115; and Department of Pathology (J.R.S.), Massachusetts General Hospital/Harvard Medical School, Boston, Massachusetts 02114

Caveolae are the major cellular membrane structure through which extracellular mediators transmit information to intracellular signaling pathways. In vascular tissue (but not ventricular myocardium), caveolin-1 (cav-1) is the main component of caveolae; cav-1 modulates enzymes and receptors, such as the endothelial nitric oxide synthase and the angiotensin II (AngII) type 1 receptor. Evidence suggests that AngII and aldosterone (ALDO) are important mediators of ventricular injury. We have described a model of biventricular damage in rodents that relies on treatment with *N*-ω-nitro-L-arginine methyl ester (L-NAME (nitric oxide synthase inhibitor)) and AngII. This damage initiated at the vascular level and was observed only in the presence of ALDO and an activated mineralocorticoid receptor (MR). We hypothesize that cav-1 modulates the adverse cardiac effects mediated by ALDO in this animal model. To test this hypothesis, we assessed the ventricular damage and measures of inflammation, in wild-type (WT) and cav-1 knockout (KO) mice randomized to either placebo or L-NAME/AngII treatment. Despite displaying cardiac hypertrophy at baseline and higher blood pressure responses to L-NAME/AngII, cav-1 KO mice displayed, as compared with WT, decreased treatment-induced biventricular damage as well as decreased transcript levels of the proinflammatory marker plasminogen activator inhibitor-1. Additionally, L-NAME/AngII induced an increase in cardiac MR levels in WT but not cav-1-ablated mice. Moreover and despite similar circulating ALDO levels in both genotypes, the myocardial damage (as determined histologically and by plasminogen activator inhibitor-1 mRNA levels) was less sensitive to ALDO levels in cav-1 KO *vs.* WT mice, consistent with decreased MR signaling in the cav-1 KO. Thus, we conclude that the L-NAME/AngII-induced biventricular damage is mediated by a mechanism partially dependent on cav-1 and signaling via MR/ALDO. **(*Endocrinology* 151: 1236–1246, 2010)**

Caveolae are important microdomains in the plasma membrane, which modulate transduction pathways via signaling molecules docked within them (1). The main component of caveolae in vascular tissues, caveolin-1 (cav-1), has been shown to associate with important modulators of cardiovascular homeostasis, such as the endothelial nitric oxide (NO) synthase (eNOS) and the angiotensin II (AngII) type 1 receptor (AT_1R) (2–9). Alterations in components of the caveolae have been shown to have profound effects both on caveolae formation and on a multitude of intracellular signaling pathways (10, 11). Thus, genetic ablation of cav-1 is accompanied, in the cardiovascular system, by cardiac hypertrophy, arterial remodeling, and alterations in vascular reactivity via an

ISSN Print 0013-7227 ISSN Online 1945-7170
Printed in U.S.A.
Copyright © 2010 by The Endocrine Society
doi: 10.1210/en.2009-0514 Received May 5, 2009. Accepted December 15, 2009.
First Published Online January 22, 2010

Abbreviations: ALDO, Aldosterone; AngII, angiotensin II; AT_1R, AngII type 1 receptor; BP, blood pressure; cav-1, caveolin-1; EC, endothelial cell; eNOS, endothelial nitric oxide synthase; FBS, fetal bovine serum; H&E, hematoxylin and eosin; HS, high sodium; KO, knockout; L-NAME, *N*-ω-nitro-L-arginine methyl ester; MDS, myocardial damage score; MR, mineralocorticoid receptor; PAI, plasminogen activator inhibitor; peNOS, phospho-eNOS; PKC, protein kinase C; SBP, systolic BP; WT, wild type.

Downloaded from https://academic.oup.com/endo/article/151/3/1236/2456616 by guest on 10 April 2024

activated NO signaling pathway (12–20). These data together support the contention that cav-1 is an important factor in maintaining cardiovascular homeostasis.

Our laboratory has extensively investigated an animal model of acute, generalized, multiple organ injury that is secondary to vascular inflammation. In this model, animals (rats and mice, the latter with and without genetic modifications) are treated with the NO synthase inhibitor *N*-[omega]-nitro-L-arginine methyl ester (L-NAME), in combination with AngII; this treatment acts via two cav-1-dependent pathways (eNOS and AT_1R) to induce significant biventricular damage initiated at the vascular level (21–23). Significantly, this damage can be prevented by mineralocorticoid receptor (MR) blockade or adrenalectomy, thus implicating aldosterone (ALDO) and its receptor as critical mediators of the cardiovascular injury (21, 22). Additionally, a variety of inflammatory factors, such as plasminogen activator inhibitor (PAI)-1 and CD-68, have been associated with such damage (23, 24).

Cell culture studies have suggested that caveolae are critical for the rapid mechanisms of action for ALDO (25). Thus, we hypothesize that cav-1 modulates the adverse cardiac effects triggered by treatment with L-NAME/AngII, and mediated by ALDO. The studies reported herein use the L-NAME/AngII model as a stressor to assess directly the interaction of cav-1 with the eNOS, AT_1R and MR, using as a distant readout the changes in myocardial damage in response to cav-1 ablation.

Materials and Methods

Animals

Twelve-week-old cav-1 knockout (KO) and genetically matched wild-type (WT) male mice (stock no. 004585 and 101045, respectively; n = 49 per genotype) were purchased from Jackson Laboratories, Bar Harbor, ME. The genotypes were confirmed by PCR, as previously described (14). Animals were housed in the animal facility in 12-h light, 12-h dark cycle at an ambient temperature of 22 ± 1 C and were maintained on *ad libitum* Purina rodent chow (5053, 0.8% NaCl; Purina, St. Louis, MO) and tap water. After 3 d of acclimatization, the mice were switched to a high-sodium (HS; 4% NaCl) diet for 5 d (d −4 to 0) at which time they had achieved sodium balance. Animals from each genotype were then randomized to two treatment groups: placebo (n = 18–20) and L-NAME/AngII (n = 29–31). All mice were maintained on the HS diet for an additional 11 d (d 1–11), throughout which they received either L-NAME (0.2 mg/ml) or placebo in the drinking water. Vehicle or AngII (Sigma-Aldrich, St. Louis, MO, 2.8 mg/kg · d) was administered on d 7–11 via Alzet osmotic sc micropumps (model 1007D; Durect Corp., Cupertino, CA). All experimental procedures followed the guidelines of and were approved by the Institutional Animal Care and Use Committee at Harvard Medical School.

Blood pressure (BP) measurements

In a preliminary study, systolic BP (SBP) was assessed simultaneously in two mice by tail-cuff plethysmography (BP analyzer, model 179; IITC LifeScience, Woodland Hills, CA; 10 measurements in each mouse) and telemetry recordings over 10 min (PA-C10 telemetry probes; Data Sciences International, St. Paul, MN), as previously reported (22, 23, 26). The readings showed excellent correlation (mouse 1: SBP 142.0 ± 17.2 and 146.5 ± 6.8 mm Hg; mouse 2: SBP 103.1 ± 7.4 and 104.2 ± 5.1 mm Hg for tail-cuff and telemetry, respectively). In the current study, SBP was determined by tail-cuff plethysmography on d 0, 7, and 11. Conscious mice were warmed at 37 C for 10 min and allowed to rest quietly before BP measurements.

Tissue preparation

At the end of the experiment, blood samples were collected, and the mice were euthanized under deep anesthesia with isoflurane, the thoracic cavity was opened, and the heart was rapidly excised and weighed. After removal of the atria, the ventricular myocardium was longitudinally divided into two halves, which were immediately placed in either liquid nitrogen (for mRNA and protein quantification) or 10% phosphate-buffered formalin (for histology analysis).

Analysis of mRNA expression by real-time RT-PCR

Total mRNA was extracted from the hearts using the RNeasy minikit (QIAGEN Sciences, Germantown, MD). cDNA was synthesized from 1.5 μg RNA with the first-strand cDNA synthesis kit (GE Healthcare, Piscataway, NJ). PCR amplification reactions were performed in duplicate, relative to 18S rRNA levels, using TaqMan gene expression assays, the ABI Prism 7000 sequence detection system (Applied Biosystems, Foster City, CA) and the ΔΔCT method. Data are presented as fold increase relative to the measurement in WT control mice (HS diet, treated with placebo).

SDS-PAGE and Western blot analysis

Protein was extracted by homogenizing cardiac tissue with radioimmunoprecipitation assay lysis buffer (Santa Cruz Biotechnology Inc., Santa Cruz, CA). Protein extracts (20 μg) were combined with an equal volume of 2× Laemmli loading buffer (containing 5% 2-mercaptoethanol), boiled for 5 min, and size fractionated by electrophoresis on 7.5–12.5% sodium dodecyl sulfate-polyacrylamide gels. Proteins were transferred from the gel to a nitrocellulose membrane by electroblotting. Membranes were incubated for 1 h with 5% nonfat dried milk in Tris-buffered saline-Tween 20 (USB Corp., Cleveland, OH) and then incubated overnight at 4 C with primary antibodies. After incubation, samples were washed, incubated with peroxidase-conjugated secondary antibody, and analyzed using enhanced chemiluminescence (Perkin-Elmer Life Sciences, Boston, MA). The blots were subsequently reprobed for β-actin, and the results were normalized to β-actin to correct for loading. Data are presented as fold change relative to the measurement in WT mice treated with L-NAME/AngII. Primary antibodies were from BD Transduction Laboratories (San Diego, CA): mouse anti-eNOS (catalog no. 610297, 1:2500), anti-cav-1 (clone 2297, catalog no. 610406, 1:1000), and anti-ERK1/2 (catalog no. 610124, 1:5000); Cell Signaling Technology (Danvers, MA): anti-protein kinase C (PKC)-δ (catalog no. 610397, 1:1000) and rabbit anti-

Downloaded from https://academic.oup.com/endo/article/151/3/1236/2456616 by guest on 10 April 2024

phospho-eNOS (peNOS) (catalog no. 9571, 1:1000); and Santa Cruz Biotechnology Inc.: rabbit anti-MR (catalog no. sc11412, 1:1000).

To evaluate eNOS dimer formation, low-temperature SDS-PAGE followed by Western blot analysis was performed according to previously published methods (27). eNOS dimer density values were normalized to total eNOS density (dimer plus monomer) from the same lane.

Immunoprecipitation

Cardiac protein extracts (500 μg) were mixed with 1 μg of corresponding primary antibody and 50 μl micromagnetic-activated cell sorting protein A or G microbeads (Miltenyi Biotec, Auburn, CA) and then incubated at 4 C for 1–2 h. The mixture was then loaded on top of Miltenyi magnetic-activated cell sorting separation columns and eluted according to manufacturer's protocol. The immunoprecipitates were then subjected to electrophoresis and analyzed as described above. In addition to the anti-cav-1 and anti-MR antibodies described above, we also used the rabbit anti-AT_1R (Santa Cruz Biotechnology) antibody (catalog no. sc1173; 1:500).

Histopathological analysis and myocardial damage score (MDS)

Cardiac tissue was fixed and embedded in paraffin blocks. Heart sections (5 μm) including both ventricles were stained with hematoxylin and eosin (H&E) and examined by light microscopy. Histopathological analysis was carried out in a blinded fashion. The MDS was determined in sections containing right and left ventricles (two to three sections per animal) using a semiquantitative scale from 0 to 4, as described (21), where 0 indicates no damage; 1, isolated myocyte damage; 2, one focal area of damage; 3, two or more areas of damage; and 4, diffuse areas of damage compromising more than 50% of the myocardium.

Plasma ALDO measurements

Blood was collected at the time the animals were killed in purple-top BD microtainer tubes (EDTA). After separation by centrifugation, plasma aldosterone levels were determined in samples with a plasma volume greater than 400 μl. Measurements were made in duplicates (200 μl each) by using a solid-phase RIA kit (Diagnostic Products Corp., Los Angeles, CA).

Primary mouse aortic endothelial cells (ECs)

Aortic ECs were isolated under sterile conditions as previously described (28, 29). Briefly, thoracic aortas were removed, rinsed, and placed in 20% fetal bovine serum (FBS)-DMEM with 1000 μg/ml heparin. The isolated aortas were then washed in serum-free DMEM containing 2 mg/ml collagenase II (Sigma-Aldrich). After 45 min incubation, ECs were removed from the aortas by flushing with 5 ml of 20% FBS-DMEM. Cells were centrifuged, resuspended, and cultured in 2 ml 20% FBS-DMEM in 35-mm collagen type I-coated dishes. After 2 h incubation at 37 C, media were removed and cells resuspended in 20% FBS-DMEM containing 100 U/ml penicillin, 100 μg streptomycin, 2 mM L-glutamine, nonessential amino acids, 1000 μg/ml sodium pyruvate (Invitrogen, Carlsbad, CA), 100 μg/ml heparin, and EC growth supplements (Sigma-Aldrich) and incubated in 5% CO_2 at 37 C in a humidified atmosphere. Cells were used at passages 2–3. The primary cultures were confirmed to be endothelial by using EC-specific markers. Confluent ECs were incubated for 5 h with the indicated concentrations of ALDO (Sigma-Aldrich) in the presence or absence of canrenoic acid (Sigma-Aldrich). After incubation, cells were lysed in radioimmunoprecipitation assay buffer and the cell lysate was analyzed for ERK1/2 and p-ERK1/2 by SDS-PAGE (10 μg protein/lane) as described above. In addition to the anti-ERK1/2 antibody (see above), we also used the rabbit anti-pERK antibody from Cell Signaling Technology (catalog no. 9101S, 1:1000).

Statistical analysis

Data are expressed as mean ± SEM. Paired data were compared by Student's *t* tests. Comparisons between multiple groups were made with one-way ANOVA followed by Tukey's *post hoc* test for multiple comparisons. Data were analyzed using the GraphPad Prism version 4.03 statistical software package (San Diego, CA). $P < 0.05$ was considered statistically significant.

Results

Cav-1 deficiency and myocardial damage

Consistent with previous reports (13), cav-1 KO mice were smaller than their WT counterparts (Table 1), despite similar food/water consumption (data not shown). Treatment with L-NAME/AngII did not influence the body weights in either genotype, throughout the experimental protocol. The cav-1 KO animals showed significantly higher heart/body weights basally, compared with the WT ($P = 0.03$, Table 1), in agreement with published data (16–20). Treatment with L-NAME/AngII induced cardiac hypertrophy in the WT mice (6.8 ± 0.4 *vs.* 5.6 ± 0.2 mg/g, L-NAME/AngII *vs.* placebo, respectively, $P = 0.009$), but the cav-1 KO mice did not significantly increase their heart to body weight ratios in response to this treatment ($P = 0.16$).

To assess the level of cardiac damage, we determined the myocardial injury semiquantitatively by scoring H&E stained tissue sections (Fig. 1, A and B). Basally, cav-1-deficient mice displayed levels of injury that were significantly ($P < 0.05$) greater than their WT counterparts (Fig. 1B, *upper panels*), in agreement with previous reports (17). The L-NAME/AngII treatment induced significant cardiac damage (areas of organizing myocardial necrosis with granulation tissue, Fig. 1B, *lower panels*) in both genotypes, with the WT animals having similar levels of damage to those previously reported by our group (21, 23). However, the injury score was significantly reduced ($P < 0.05$) in the cav-1-deficient mice, compared with the WT. Similar responses were obtained for the proinflammatory marker PAI-1 and the macrophage-specific marker CD-68 ($P < 0.05$), assessed at the cardiac mRNA levels (Fig. 1, C and D).

Downloaded from https://academic.oup.com/endo/article/151/3/1236/2456616 by guest on 10 April 2024

TABLE 1. Body weights (BW), heart weights (HW), HW to BW ratios, SBP levels, and SBP variation in WT and cav-1 KO mice: effect of treatment with L-NAME and AngII

		cav-1 WT		cav-1 KO	
	Day	Control	L-NAME/AngII	Control	L-NAME/AngII
BW (g)	0	27.9 ± 0.7 (21)	28.4 ± 0.4 (29)	24.8 ± 0.7 (18)[a]	24.7 ± 0.5 (25)[a]
	11	27.1 ± 0.6 (18)	28.5 ± 1.2 (25)	23.9 ± 0.5 (18)[a]	24.8 ± 1.1 (18)[a]
HW (mg)	11	151 ± 4.7 (21)	185 ± 6.2 (26)[b]	148 ± 5.8 (18)	165 ± 7.3 (18)[a]
HW to BW (mg/g)	11	5.8 ± 0.2 (21)	6.8 ± 0.4 (26)[b]	6.2 ± 0.2 (18)[a]	6.8 ± 0.4 (18)
SBP (mm Hg)	0	109 ± 2.7 (20)	111 ± 1.8 (29)	114 ± 3.1 (18)	114 ± 2.2 (31)
	7	113 ± 2.3 (20)	127 ± 3.5 (29)[b,c]	121 ± 2.1 (18)[a]	141 ± 3.6 (31)[a,b,c]
	11	116 ± 0.9 (18)	159 ± 4.7 (24)[d,e]	121 ± 1.8 (18)[a]	169 ± 4.8 (20)[a,d,e]
ΔSBP (mm Hg)	7-0	0.9 ± 3.3 (18)	15.9 ± 3.0 (29)[b]	7.1 ± 3.9 (18)	27.2 ± 4.0 (31)[a,b]
	11-7	1.7 ± 2.6 (18)	28.9 ± 6.0 (24)[b]	0.0 ± 3.2 (16)	24.3 ± 7.0 (20)[b]
	11-0	8.4 ± 2.5 (16)	47.3 ± 5.4 (24)[d]	6.7 ± 3.8 (16)	55.8 ± 4.8 (20)[d]

Data are provided as average ± SEM (number of animals).

[a] $P < 0.05$ *vs.* corresponding treatment and time point in cav-1 WT mice; [b] $P < 0.01$ *vs.* control animals of the same genotype; [c] $P < 0.001$ *vs.* d 0 in animals of the same genotype and treatment; [d] $P <$ 1.E-05 *vs.* control animals of the same genotype; [e] $P <$ 1.E-13 *vs.* d 0 in animals of the same genotype and treatment.

Cav-1 deficiency and the BP response to L-NAME/AngII

Because BP is an important contributor to cardiac hypertrophy and myocardial damage (30, 31), we assessed whether differences in BP responses to L-NAME/AngII could explain the reduced cardiac injury in the cav-1 KO mice (Table 1). Animals treated with placebo did not change their BP over the course of the experiment; however, cav-1 KO control animals tended to have higher BP levels at d 7 and 11, compared with WT mice. Before treatment, basal SBP was similar in WT and cav-1 KO mice; after 7 d of L-NAME treatment, the SBP was significantly increased in both genotypes. Interestingly, eNOS inhibition for 7 d induced a significantly greater change in BP in the cav-1 KO, compared with WT mice ($P < 0.03$), as expected for an animal with an activated NO system (12, 13). The addition of AngII to the treatment for an additional 4 d induced a further SBP increase, similar in both genotypes (Table 1). These data are consistent with intact AT_1R signaling in the L-NAME-treated, cav-1-deficient mice. After 11 d of combined L-NAME/AngII treatment, the final BP levels were significantly higher in the cav-1 KO, compared with WT mice (Table 1). Our data suggest that the differential effect of L-NAME/AngII treatment on BP levels in cav-1 KO and WT mice is likely due to the effects of cav-1 ablation on eNOS. Additionally, these data suggest that the L-NAME/AngII-induced cardiac injury was less dependent on BP in cav-1 KO, compared with WT mice.

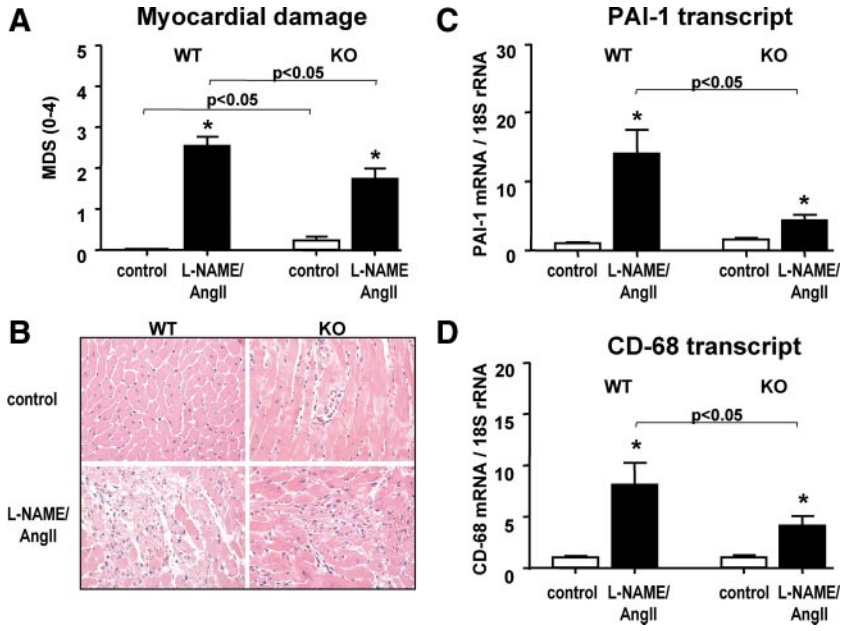

FIG. 1. Myocardial damage and inflammatory markers in cav-1 WT and KO mice. A, MDSs were determined in heart tissues obtained from placebo- (control) or L-NAME/AngII-treated animals (n > 18/group). B, Representative H&E staining of myocardial tissue sections from cav-1 WT (*left panels*) and KO (*right panels*) animals, treated with either placebo (*upper panels*) or L-NAME/AngII (*lower panels*). Magnification, ×400. C and D, Heart tissues were analyzed by real-time RT-PCR for PAI-1 (C, n > 11/group) and CD-68 (D, n > 8/group) levels, as described in *Materials and Methods*. *, $P < 0.01$ *vs.* control animals of the same genotype.

Effect of L-NAME/AngII and cav-1 deletion on eNOS

Because eNOS is directly affected by L-NAME treatment and the cav-1 KO was reported to display increased NO levels (16), we first analyzed the cardiac levels of eNOS. The L-NAME/AngII treatment resulted in higher levels of eNOS and peNOS protein in the WT cardiac tissue; however, no significant increases were observed for the KO ani-

Downloaded from https://academic.oup.com/endo/article/151/3/1236/2456616 by guest on 10 April 2024

mals, despite significantly higher levels of eNOS and peNOS at baseline ($P < 0.001$, Fig. 2, A and B). These data suggest an altered NO response mechanism to damage in the cav-1-deficient mice, consistent with the greater SBP response to L-NAME in these animals (Table 1). Another approach to detect eNOS activation is by assessing its presence in the dimer form, which is the NO-producing form of eNOS under physiological conditions (32). Western analysis under nonreducing conditions showed that treatment with L-NAME/AngII induced a significant increase in eNOS dimerization in the WT but not the cav-1 KO mice (Fig. 2C). These data together are consistent with an impaired eNOS coupling and subsequent activation in response to L-NAME/AngII in the cav-1-deficient heart.

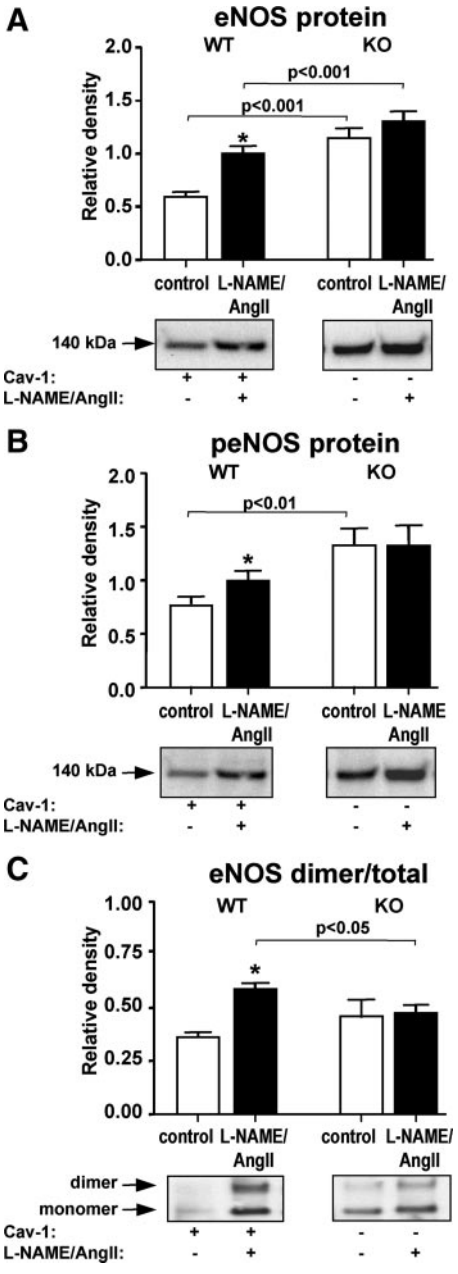

FIG. 2. eNOS expression in cav-1 WT and KO mice. Heart tissues from animals treated with placebo (control) or L-NAME/AngII were analyzed by Western blotting under denaturing (A and B) or nondenaturing (C) conditions, as described in *Materials and Methods*, using total eNOS (A and C) and phospho-eNOS (Ser1177) antibodies (B), respectively. Representative Western blots are depicted under each bar graph. *, $P < 0.001$ *vs.* control animals of the same genotype.

Cav-1 deficiency and caveolar protein complexes in the mouse heart

Our L-NAME/AngII-induced model of damage relies on eNOS, AT_1R, and MR signaling (21–23). It has been documented that the scaffolding domain of caveolin binds caveolin-binding motifs of the type $\phi X\phi XXXX\phi$, $\phi XXXX\phi XX\phi$, or $\phi X\phi XXXX\phi XX\phi$, where ϕ is an aromatic or Leu residue and X any amino acid (2); such motifs are present in almost all signaling proteins that bind caveolins, including eNOS and the AT_1R (2–7). The relationship between cav-1 and eNOS has been well studied by several groups (2–4); however, caveolae seem to be a critical modulator also for AngII- and ALDO-mediated rapid effects in cell culture (6, 7, 25). Therefore, we examined the relationship between cav-1 and the AT_1R and MR. We first assessed whether a caveolin-binding motif was present in the MR; protein sequence analysis showed that the MR contains such a motif (Fig. 3A), situated in the middle of the N-terminal domain between amino acids 450 and 460 (FPFMDGSYFSF) and highly conserved in several species, including human, mouse, and rat. This

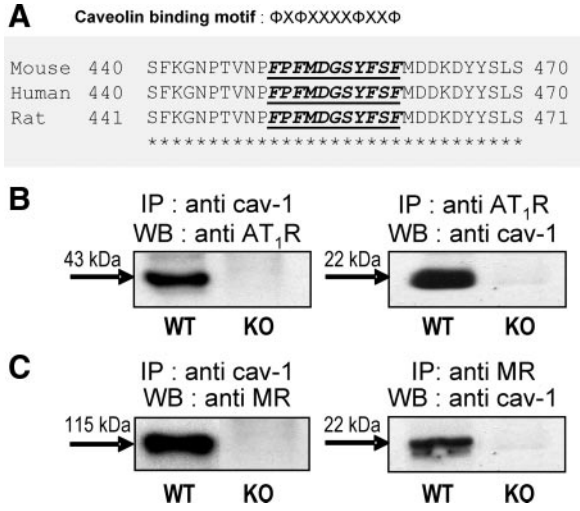

FIG. 3. A, cav-1 binding motif within MR sequence. A putative cav-1 binding motif is located in the midportion of the N-terminal region of the MR. Sequence alignment between mouse, human, and rat MR shows that this region is highly conserved between species. ϕ, Aromatic amino residues Trp, Phe, or Try; X, any amino acid. B and C, Coimmunoprecipitation patterns for cav-1, AT_1R, and MR in mouse hearts. Representative Western blots (WB) showing reciprocal immunoprecipitation (IP) of cav-1 with the AT_1R and MR. Tissue homogenates from WT and cav-1 KO mice were immunoprecipitated with anti-cav-1 (B and C, *left panels*), anti-AT_1R (B, *right panel*), anti-MR (C, *right panel*) and then analyzed by Western blotting for the presence of AT_1R (B, *left panel*), cav-1 (B and C, *right panel*), and MR (C, *left panel*), respectively, as described in *Materials and Methods*.

Downloaded from https://academic.oup.com/endo/article/151/3/1236/2456616 by guest on 10 April 2024

suggested that an interaction between the MR and cav-1 would be possible via this motif. To verify the likelihood that these proteins could associate *in vivo*, we conducted immunoprecipitation experiments in heart tissues from WT and cav-1 KO mice. As shown in Fig. 3, both the AT_1R and the MR coimmunoprecipitated with cav-1 in heart tissues from WT animals, but, as expected, the cav-1/MR complexes were absent in cav-1-deficient tissues (Fig. 3, B and C). Additional data supporting the existence of a cav-1/MR complex not only in mouse but also in rat and human tissues is presented in the data supplement (Supplemental Methods, Supplemental References, and Supplemental Figs. 1–4) published on The Endocrine Society's Journals Online web site at http://endo.endojournals.org; thus, we have shown that MR and cav-1 colocalize in rat cardiac and renal vessels (Supplemental Fig. 1) and coimmunoprecipitate in EA.hy926 human ECs as well as rat heart tissue (Supplemental Fig. 2). The specificity of this interaction was verified by the use of different anti-cav-1 and anti-MR antibodies (Supplemental Figs. 2–4) as well as negative (Supplemental Fig. 3) and positive controls (Supplemental Fig. 4). Thus, the existence of cav-1 complexes with both the AT_1R and the MR suggests that, in cav-1-deficient animals, the AT_1R- and MR-mediated mechanisms may be affected, possibly altering the levels of cardiac damage induced by L/NAME/AngII treatment.

Effect of L-NAME/AngII and cav-1 deletion on the AT_1R and downstream signaling pathways

The cardiac levels of AT_1R transcript in WT and cav-1 KO mice were similar basally and were significantly down-regulated in response to L-NAME/AngII, as expected in a model of excess AngII (Fig. 4A). Early vascular inflammatory processes that are induced by activating the AngII pathway or inhibiting NO production are associated with the activation of the PKCδ/ERK1/2 cascade (33–38). We assessed the protein levels of cardiac PKCδ and ERK1/2; our analysis showed that ERK1/2 and PKCδ levels were increased in the L-NAME/AngII- *vs.* placebo-treated groups, with no significant effect of cav-1 ablation (Fig. 4, B and C). These data confirm that the AT_1R, PKCδ, and ERK1/2 levels are modulated by treatment with L-NAME/AngII, with cav-1 not being a critical modulator of this signaling pathway. The disconnect between the reduced cardiac inflammation (Fig. 1) and unchanged AT_1R, PKCδ, and ERK1/2 levels in KO *vs.* WT animals suggests that in the absence of cav-1, a different cardiovascular inflammatory pathway may be modified.

Effect of L-NAME/AngII and cav-1 deletion on the MR and plasma ALDO levels

We previously documented that the L-NAME/AngII-induced damage in our model was mediated by ALDO and

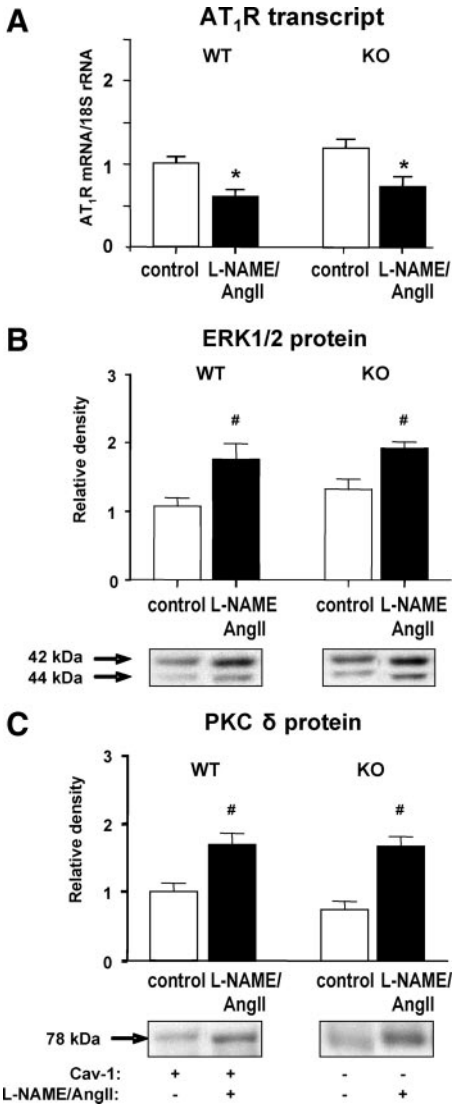

FIG. 4. Effect of L-NAME/AngII treatment on AT_1R transcript levels and ERK1/2 and PKCδ protein expression in cav-1 WT and KO mouse hearts. Heart tissues from animals treated with placebo (control) or L-NAME/AngII were analyzed by real-time RT-PCR (A) or Western blotting (B and C), as described in *Materials and Methods*. Representative Western blots are depicted *under each bar graph* (B and C). *, $P < 0.01$; #, $P < 0.05$ *vs.* control animals of the same genotype.

an activated MR (21, 23). Consistent with those data, Fig. 5A shows that treatment with L-NAME/AngII significantly increased plasma ALDO in both WT and cav-1 KO animals. However, there were no significant differences between the ALDO levels in the two genotypes. Cardiac MR protein levels were significantly up-regulated in response to L-NAME/AngII-treatment in the WT ($P < 0.01$) but not the cav-1 KO mice (Fig. 5B), despite similar baseline MR levels in the two genotypes (Fig. 5B). These data together raise the possibility that the decreased cardiac damage observed in the cav-1 KO be correlated with an impaired ALDO/MR signaling in the cav-1-deficient heart.

To assess the effect of cav-1 ablation on the relationship between ALDO/MR and the ventricular damage, we an-

Downloaded from https://academic.oup.com/endo/article/151/3/1236/2456616 by guest on 10 April 2024

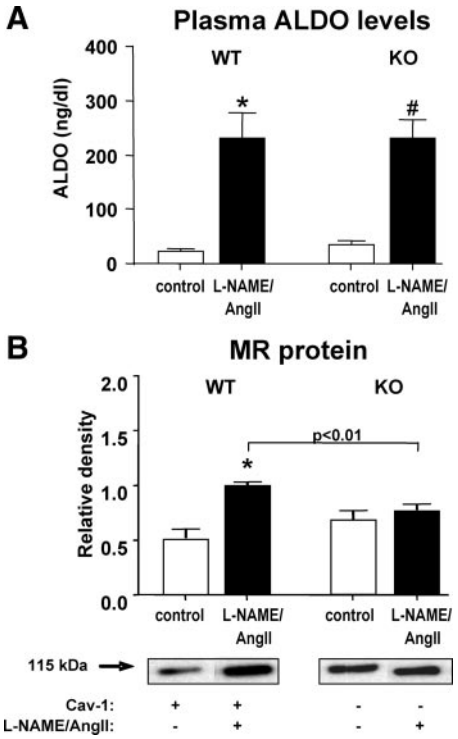

FIG. 5. Effect of L-NAME/AngII treatment on ALDO and MR protein levels in cav-1 WT and KO mouse hearts. Plasma ALDO levels (A) were determined in placebo- and L-NAME/AngII-treated mice, as described in *Materials and Methods*. Heart tissues from animals treated with placebo (control) or L-NAME/AngII were analyzed by Western blotting for MR protein levels (B), as described in *Materials and Methods*. Representative Western blots are depicted under the bar graph (B). *, $P < 0.001$; #, $P < 1.E\text{-}05$ *vs.* control animals of the same genotype.

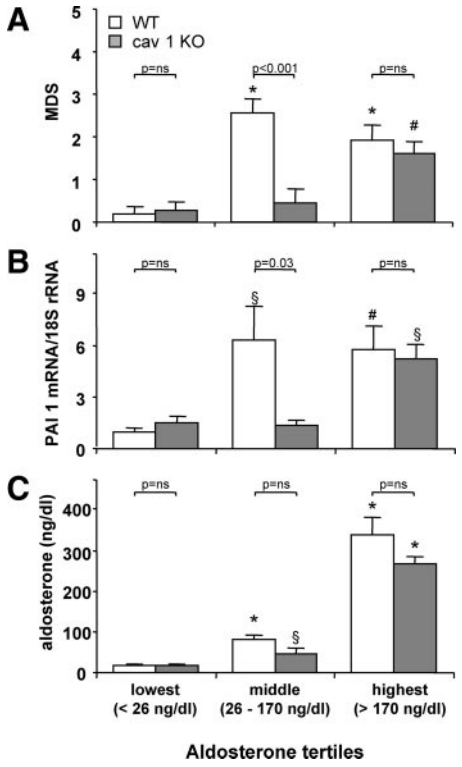

FIG. 6. Myocardial damage scores and PAI-1 expression are dependent on ALDO tertiles in cav-1 WT and cav-1 KO mice. Myocardial damage scores (A) and cardiac PAI-1 transcript levels (B) were determined in a subset of WT and cav-1 KO mice (after placebo or L-NAME/AngII treatment), for which ALDO levels were also available (C). Data were grouped by plasma ALDO levels tertiles (<26 ng/dl, ≥26 ng/dl, but <170 ng/dl, and >170 ng/dl). ALDO levels for WT and cav-1 KO within each tertile were not different from each other (C). *, $P < 0.0001$; #, $P < 0.01$; §, $P < 0.05$ *vs.* animals with the same genotype and ALDO levels in the lowest tertile.

alyzed the myocardial injury scores by tertiles of plasma ALDO levels in a subset of placebo- and L-NAME/AngII-treated WT and cav-1 KO mice for which both myocardial damage and ALDO levels were available (Fig. 6A). No significant differences were observed between WT and cav-1 KO mice in the lowest and highest tertiles (ALDO <26 ng/dl and ALDO >170 ng/dl, respectively). However, WT mice in the middle ALDO tertile (ALDO levels between 26 and 170 ng/dl) had significantly higher myocardial injury levels, compared with cav-1 KO mice ($P = 0.0004$). Similar results were obtained for the proinflammatory marker PAI-1 (Fig. 6B) and the macrophage-specific marker CD-68 (not shown). These data suggest that the cav-1 KO myocardium is less sensitive to the detrimental effects of ALDO, likely due to an altered MR signaling in the heart, in the absence of cav-1, consistent with the existence of an MR/cav-1 complex that modulates the effects of L-NAME/AngII treatment in the cardiac vasculature.

Effect of cav-1 deletion on endothelial cells response to ALDO

To determine whether the ALDO/MR signaling is altered in the absence of cav-1, we assessed the levels of ERK1/2 (total and phosphorylated) in response to ALDO, in primary vascular ECs isolated from cav-1 KO and WT mouse aortas. As shown in Fig. 7, 5 h treatment with ALDO induced a substantial increase in pERK to ERK ratio that was significantly greater in the WT than the cav-1 KO ECs. These results suggest that the absence of cav-1 reduces the responsiveness of these cells to ALDO, thereby supporting the indirect evidence provided in our *in vivo* studies. Furthermore, the fact that the MR antagonist canrenoate was equally effective in the two cell types supports this conclusion.

Discussion

Caveolae are dynamic regulators of receptor-induced signal transduction (1). Structurally they are maintained by a scaffold of caveolin molecules that anchor receptors and enzymes via direct interaction with cav-1 (in most tissues) or cav-3 (in skeletal muscle and myocytes) (39). This study was designed to test the hypothesis that cav-1 modulates the adverse cardiovascular effects mediated by ALDO using the L-NAME/AngII model. We documented that cav-1

Downloaded from https://academic.oup.com/endo/article/151/3/1236/2456616 by guest on 10 April 2024

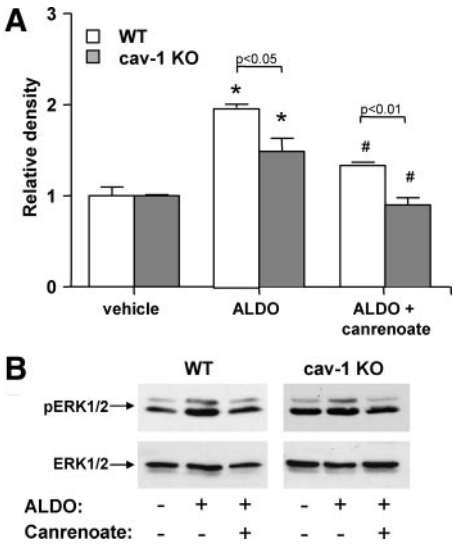

FIG. 7. ALDO-induced ERK1/2 phosphorylation in ECs is reduced in the absence of cav-1. A, Primary aortic ECs were isolated from WT and cav-1 KO mice, grown for two to three passages and incubated with vehicle or 10^{-8} M aldosterone in the presence or absence of 10^{-6} M MR antagonist canrenoate. Five hours later, cells were lysed and analyzed for the levels of total and phosphorylated ERK1/2. Data were normalized to results obtained in WT cells treated with vehicle. B, Representative Western blots showing pERK1/2 (*top panels*) and total ERK1/2 levels (*bottom panels*) in WT (*left panels*) and cav-1 KO ECs (*right panels*), treated with vehicle (first lanes) or ALDO in the absence (second lanes) or presence of canrenoate (third lanes). *, $P < 0.001$ *vs.* vehicle-treated cells of the same genotype; #, $P < 0.01$ *vs.* ALDO-treated cells of the same genotype.

deficiency is associated with a significant reduction in L-NAME/AngII-induced biventricular damage and inflammation (Fig. 1), despite the greater BP response to treatment displayed by the cav-1 KO *vs.* WT mice (Table 1). Additionally and despite similar circulating ALDO levels, the myocardial damage (as assessed by cardiac histology and PAI-1 transcript levels) was less sensitive to ALDO levels in the cav-1 KO, compared with WT mice (Fig. 6). This presumed decreased sensitivity was directly tested in the cav-1-deficient primary ECs with positive confirmation (Fig. 7). From additional data, the proposed mechanism underlying this decreased sensitivity is a failure of MR levels to appropriately increase in response to treatment with L-NAME/AngII in the absence of cav-1 (Fig. 5). Together these findings support our hypothesis that the cav-1/MR complex (Fig. 3) is a major player involved in mediating the detrimental effects of L-NAME/AngII in the heart and raises the possibility that this cav-1/MR effect may mediate cardiovascular damage in general.

There is growing evidence that cav-1 plays an important role in cardiovascular damage. Previous reports have shown a cardiovascular phenotype associated with cav-1 deficiency at baseline that includes cardiac hypertrophy and dysfunction (16–20) as well as vascular remodeling with altered vasoreactivity (12–15). Our data extend these observations under baseline conditions to include an increased cardiac inflammatory milieu in the cav-1 KO mouse.

Previous studies suggested that the actions of eNOS may be mediated by cav-1 (2–4). Our results herein support this contention; thus, 1 wk of L-NAME treatment induced a significantly greater change in SBP in the cav-1 KO, compared with WT (Table 1) that is consistent with an activated NO system in the cav-1-ablated animals (12–14, 16). Our findings are supported by a recent report showing greater SBP increases in the cav-1 KO than the WT after treatment with L-NAME postnatally for 2 months (40). Additionally, we documented that the levels of cardiac eNOS (both total and Ser1177 phosphorylated) were significantly greater at baseline in the cav-1 KO animal (Fig. 2). Because the baseline BP levels were not different between the two genotypes, it is conceivable that the cav-1-deficient animals activate a compensatory mechanism to counteract the hypotensive effect of systemic NO levels that could be as much as 5-fold higher than in the WT (16). Our elevated peNOS levels in the KOs further support this observation. However, excessive NO production can have both beneficial and adverse effects on the myocardium, as demonstrated in both human and animal models (41). Thus, it is likely that the baseline cardiac hypertrophy and inflammatory damage observed in the cav-1 KO mice are, at least in part, due to an overexpressed or hyperactivated eNOS system.

The biventricular damage observed in our animal model (rodents treated with L-NAME/AngII) was shown to be, in part, secondary to vascular inflammation (21–23). cav-1 is the major caveolin that mediates the effects of both eNOS and AngII in vascular tissues (2–9) but not ventricular myocytes; it was therefore not surprising that the myocardial damage in L-NAME/AngII-treated mice (Fig. 1) was reduced in cav-1 KO when compared with their WT counterparts. We have shown that the eNOS abundance, phosphorylation, and dimerization were increased in response to L-NAME/AngII in WT but not KO animals. These findings are consistent with vascular cav-1 being an important mediator of eNOS coupling and phosphorylation in response to L-NAME/AngII treatment, despite its down-regulating role in baseline conditions. Because L-NAME is an inhibitor of eNOS dimer formation (42), it is likely that the L-NAME/AngII-mediated eNOS dimerization we observed in WT mice is mostly a response to AngII stimulation. Thus, it appears that the relatively protective effect of cav-1 ablation may be, in part, due to an impaired eNOS activation mechanism, consistent with the documented effect of L-NAME on improving heart function in the cav-1-deficient animals (40).

Interestingly, cav-1 ablation did not appear to modify the way in which treatment with L-NAME/AngII affects

Downloaded from https://academic.oup.com/endo/article/151/3/1236/2456616 by guest on 10 April 2024

the levels of AT_1R and its downstream transduction molecules, ERK1/2 and PKCδ (33–38), despite the disruption of the cav-1/AT_1R complex. Moreover, the addition of AngII to the L-NAME treatment induced a similar increase in SBP levels in both genotypes, consistent with a functional AngII/AT_1R pathway in the absence of cav-1. This hypothesis is supported by our data showing that the baseline and AngII-stimulated ALDO levels were indistinguishable between the cav-1 KO and WT animals (Fig. 5). Previous cell culture studies established that the interaction between cav-1 and the AT_1R is dynamic: whereas cav-1 does not dock the unstimulated AT_1R to caveolae, it is a necessary partner for AT_1R trafficking on AngII stimulation (6–9). Two possible explanations may reconcile the apparent discrepancy between these studies and our data. First, the regulation of AT_1R expression levels in the cardiac tissue may likely be independent of the AT_1R trafficking to caveolae. Second, the effect of AT_1R stimulation (including ERK1/2 and PKCδ up-regulation) in our model may be due to direct AngII actions on the cav-1-free ventricular myocytes and not on the vasculature. Indeed, it has been shown that the AngII-induced cardiac damage in mice can be mediated by direct effects on the cardiomyocyte AT_1R (43). Additionally, the effects of AngII stimulation on SBP may be mediated by cav-3 complexes in the vascular smooth muscle layer (44). Thus, in the absence of cav-1, the primary signaling pathway for our model of damage may be mediated by a cav-1-independent AT_1R activation mechanism.

Previous results from our laboratory demonstrated that ALDO and MR are important mediators of the L-NAME/AngII-induced cardiovascular injury (21, 22). Consistent with these findings, the cav-1/MR complex identified in the present study (Fig. 3) appears to play an important role in mediating the effects of L-NAME/AngII on the heart. Plasma ALDO levels in the middle tertile (Fig. 6) were associated with significant myocardial damage and inflammation in the WT but not the cav-1-deficient animals, consistent with an ALDO-MR interaction that is shifted to the right in these animals. This finding is consistent with at least one of four possibilities for this genotype: 1) lower MR levels in the presence of ALDO-inducing treatment; 2) lower ALDO levels; 3) modified coupling between ALDO and MR in the absence of cav-1, resulting in altered downstream signaling; or 4) the presence of an endogenous inhibitor. Indeed, the MR levels failed to increase in response to L-NAME/AngII in the cav-1 KO mouse (Fig. 5), despite similar levels of circulating ALDO (Figs. 5 and 6); thus, our data support the conclusion that the MR is less sensitive to ALDO levels in the cav-1 KO. Alternatively, because ALDO levels could be a biomarker for the effects of AngII, Fig. 6 could also be interpreted as dissociation between AngII levels and myocardial damage/inflammation. However, as discussed above, our data suggest that the AT_1R signaling is not a significant contributor to the differences observed between the L-NAME/AngII-induced damage in WT and cav-1 KO.

The cav-1-rich caveolae have been described as docking sites for other steroid receptors, such as the estrogen receptor-α and androgen receptor (45–47), that interact with cav-1 in a ligand-dependent or -independent manner. The cav-1/MR interaction identified herein is most likely mediated via the evolutionary conserved cav-1 binding motif in the MR sequence. Interestingly, this motif is situated in the N-terminal portion of the MR, distal to the C-terminal EF domains that were recently shown to mediate the nongenomic effects of the MR (48). This intriguing finding supports the hypothesis that in addition to the traditional nuclear role for MR, this receptor may also have a membrane-related one. This is consistent with previous reports in cell culture experiments, which ALDO stimulation resulted in a shift of cav-1 to denser regions of the plasma membrane (49). In agreement with these results, it has been suggested that caveolae are critical for the rapid mechanisms of action for ALDO in cell culture (25). Our studies in primary ECs isolated from WT and cav-1 KO mouse aortas (Fig. 7) are consistent with the ALDO-induced MR activation being impaired in the absence of cav-1. Because both cell types are equally responsive to canrenoate, it is unlikely that our results are secondary to the generation of an endogenous antagonist or an alteration in the MR structure in the cav-1 KO. Thus, our results are best explained by a process that is independent of the MR *per se* and dependent on an interaction between MR and cav-1. Further studies are, however, needed to determine the potential mechanisms involved in the cav-1-dependent MR signaling.

In summary, we conclude that the relative protective effect of cav-1 KO against L-NAME/AngII-induced cardiovascular damage is likely secondary to several factors: 1) increased eNOS basally, 2) loss of L-NAME/AngII-induced eNOS phosphorylation and dimerization, and 3) a reduction in the activity of the ALDO/MR pathway. Furthermore, this relative protection in response to acute injury was not due to differences in serum ALDO or the activation of the AT_1R pathway. Thus, our study provides evidence that cav-1 may have a deleterious role in mediating cardiovascular damage, in part, by modulating signaling via the MR/ALDO pathway.

Acknowledgments

Address all correspondence and requests for reprints to: Gordon H. Williams, M.D., Brigham and Women's Hospital/Harvard

Downloaded from https://academic.oup.com/endo/article/151/3/1236/2456616 by guest on 10 April 2024

Medical School, Department of Endocrinology, Diabetes, and Hypertension, 221 Longwood Avenue, Boston, Massachusetts 02115. E-mail: gwilliams@partners.org.

This work was supported by National Institutes of Health Grants 5T32HL007609 (to L.H.P. and C.G.), IL096518 and ES014462 (to J.R.R.), HL63423 (to G.K.A.), and HL069208 (to G.H.W.). L.H.P. is supported by a Scientist Development Grant from the American Heart Association (0735609T).

Disclosure Summary: The authors have nothing to declare.

References

1. **Frank PG, Hassan GS, Rodriguez-Feo JA, Lisanti MP** 2007 Caveolae and caveolin-1: novel potential targets for the treatment of cardiovascular disease. Curr Pharm Des 13:1761–1769
2. **Couet J, Li S, Okamoto T, Ikezu T, Lisanti MP** 1997 Identification of peptide and protein ligands for the caveolin-scaffolding domain. Implications for the interaction of caveolin with caveolae-associated proteins. J Biol Chem 272:6525–6533
3. **García-Cardeña G, Martasek P, Masters BS, Skidd PM, Couet J, Li S, Lisanti MP, Sessa WC** 1997 Dissecting the interaction between nitric oxide synthase (NOS) and caveolin. Functional significance of the nos caveolin binding domain *in vivo*. J Biol Chem 272:25437–25440
4. **Li H, Brodsky S, Basco M, Romanov V, De Angelis DA, Goligorsky MS** 2001 Nitric oxide attenuates signal transduction: possible role in dissociating caveolin-1 scaffold. Circ Res 88:229–236
5. **Ishizaka N, Griendling KK, Lassègue B, Alexander RW** 1998 Angiotensin II type 1 receptor: relationship with caveolae and caveolin after initial agonist stimulation. Hypertension 32:459–466
6. **Wyse BD, Prior IA, Qian H, Morrow IC, Nixon S, Muncke C, Kurzchalia TV, Thomas WG, Parton RG, Hancock JF** 2003 Caveolin interacts with the angiotensin II type 1 receptor during exocytic transport but not at the plasma membrane. J Biol Chem 278:23738–23746
7. **Ushio-Fukai M, Alexander RW** 2006 Caveolin-dependent angiotensin II type 1 receptor signaling in vascular smooth muscle. Hypertension 48:797–803
8. **Olivares-Reyes JA, Shah BH, Hernández-Aranda J, García-Caballero A, Farshori MP, García-Sáinz JA, Catt KJ** 2005 Agonist-induced interactions between angiotensin AT1 and epidermal growth factor receptors. Mol Pharmacol 68:356–364
9. **Leclerc PC, Auger-Messier M, Lanctot PM, Escher E, Leduc R, Guillemette G** 2002 A polyaromatic caveolin-binding-like motif in the cytoplasmic tail of the type 1 receptor for angiotensin II plays an important role in receptor trafficking and signaling. Endocrinology 143:4702–4710
10. **Hnasko R, Lisanti MP** 2003 The biology of caveolae: lessons from caveolin knockout mice and implications for human disease. Mol Interv 3:445–464
11. **Cohen AW, Hnasko R, Schubert W, Lisanti MP** 2004 Role of caveolae and caveolins in health and disease. Physiol Rev 84:1341–1379
12. **Drab M, Verkade P, Elger M, Kasper M, Lohn M, Lauterbach B, Menne J, Lindschau C, Mende F, Luft FC, Schedl A, Haller H, Kurzchalia TV** 2001 Loss of caveolae, vascular dysfunction, and pulmonary defects in caveolin-1 gene-disrupted mice. Science 293:2449–2452
13. **Razani B, Engelman JA, Wang XB, Schubert W, Zhang XL, Marks CB, Macaluso F, Russell RG, Li M, Pestell RG, Di Vizio D, Hou Jr H, Kneitz B, Lagaud G, Christ GJ, Edelmann W, Lisanti MP** 2001 Caveolin-1 null mice are viable but show evidence of hyperproliferative and vascular abnormalities. J Biol Chem 276:38121–38138
14. **Pojoga LH, Yao TM, Sinha S, Ross RL, Lin JC, Raffetto JD, Adler GK, Williams GH, Khalil RA** 2008 Effect of dietary sodium on vasoconstriction and eNOS-mediated vascular relaxation in caveolin-1 deficient mice. Am J Physiol Heart Circ Physiol 294:H1258–H1265
15. **Albinsson S, Shakirova Y, Rippe A, Baumgarten M, Rosengren BI, Rippe C, Hallmann R, Hellstrand P, Rippe B, Swärd K** 2007 Arterial remodeling and plasma volume expansion in caveolin-1-deficient mice. Am J Physiol Regul Integr Comp Physiol 293:R1222–R1231
16. **Zhao YY, Liu Y, Stan RV, Fan L, Gu Y, Dalton N, Chu PH, Peterson K, Ross Jr J, Chien KR** 2002 Defects in caveolin-1 cause dilated cardiomyopathy and pulmonary hypertension in knockout mice. Proc Natl Acad Sci USA 99:11375–11380
17. **Cohen AW, Park DS, Woodman SE, Williams TM, Chandra M, Shirani J, Pereira de Souza A, Kitsis RN, Russell RG, Weiss LM, Tang B, Jelicks LA, Factor SM, Shtutin V, Tanowitz HB, Lisanti MP** 2003 Caveolin-1 null mice develop cardiac hypertrophy with hyperactivation of p42/44 MAP kinase in cardiac fibroblasts. Am J Physiol Cell Physiol 284:C457–C474
18. **Park DS, Cohen AW, Frank PG, Razani B, Lee H, Williams TM, Chandra M, Shirani J, De Souza AP, Tang B, Jelicks LA, Factor SM, Weiss LM, Tanowitz HB, Lisanti MP** 2003 Caveolin-1 null (−/−) mice show dramatic reductions in life span. Biochemistry 42:15124–15131
19. **Wunderlich C, Schober K, Lange SA, Drab M, Braun-Dullaeus RC, Kasper M, Schwencke C, Schmeisser A, Strasser RH** 2006 Disruption of caveolin-1 leads to enhanced nitrosative stress and severe systolic and diastolic heart failure. Biochem Biophys Res Commun 340:702–708
20. **Murata T, Lin MI, Huang Y, Yu J, Bauer PM, Giordano FJ, Sessa WC** 2007 Reexpression of caveolin-1 in endothelium rescues the vascular, cardiac, and pulmonary defects in global caveolin-1 knockout mice. J Exp Med 204:2373–2382
21. **Rocha R, Stier Jr CT, Kifor I, Ochoa-Maya MR, Rennke HG, Williams GH, Adler GK** 2000 Aldosterone: a mediator of myocardial necrosis and renal arteriopathy. Endocrinology 141:3871–3878
22. **Martinez DV, Rocha R, Matsumura M, Oestreicher E, Ochoa-Maya M, Roubsanthisuk W, Williams GH, Adler GK** 2002 Cardiac damage prevention by eplerenone: comparison with low sodium diet or potassium loading. Hypertension 39:614–618
23. **Oestreicher EM, Martinez-Vasquez D, Stone JR, Jonasson L, Roubsanthisuk W, Mukasa K, Adler GK** 2003 Aldosterone and not plasminogen activator inhibitor-1 is a critical mediator of early angiotensin II/NG-nitro-L-arginine methyl ester-induced myocardial injury. Circulation 108:2517–2523
24. **Schneider M, Kostin S, Strøm CC, Aplin M, Lyngbaek S, Theilade J, Grigorian M, Andersen CB, Lukanidin E, Lerche Hansen J, Sheikh SP** 2007 S100A4 is upregulated in injured myocardium and promotes growth and survival of cardiac myocytes. Cardiovasc Res 75:40–50
25. **Callera GE, Montezano AC, Yogi A, Tostes RC, Touyz RM** 2007 Vascular signaling through cholesterol-rich domains: implications in hypertension. Curr Opin Nephrol Hypertens 16:90–104
26. **Guo C, Martinez-Vasquez D, Mendez GP, Toniolo MF, Yao TM, Oestreicher EM, Kikuchi T, Lapointe N, Pojoga L, Williams GH, Ricchiuti V, Adler GK** 2006 Mineralocorticoid receptor antagonist reduces renal injury in rodent models of types 1 and 2 diabetes mellitus. Endocrinology 147:5363–5373
27. **Venema RC, Ju H, Zou R, Ryan JW, Venema VJ** 1997 Subunit interactions of endothelial nitric-oxide synthase. Comparisons to the neuronal and inducible nitric-oxide synthase isoforms. J Biol Chem 272:1276–1282
28. **Kobayashi M, Inoue K, Warabi E, Minami T, Kodama T** 2005 A simple method of isolating mouse aortic endothelial cells. J Atheroscler Thromb 12:138–142
29. **Dame MK, Yu X, Garrido R, Bobrowski W, McDuffie JE, Murphy HS, Albassam M, Varani J** 2003 A stepwise method for the isolation of endothelial cells and smooth muscle cells from individual canine coronary arteries. In Vitro Cell Dev Biol Anim 39:402–406

Downloaded from https://academic.oup.com/endo/article/151/3/1236/2456616 by guest on 10 April 2024

30. **Cardillo C, De Felice F, Campia U, Musumeci V, Folli G** 1996 Relation of stress testing and ambulatory blood pressure to hypertensive cardiac damage. Am J Hypertens 9:162–170
31. **Morgan TO, Aubert JF, Wang Q** 1998 Sodium, angiotensin II, blood pressure, and cardiac hypertrophy. Kidney Int Suppl 67: S213–S215
32. **Förstermann U, Münzel T** 2006 Endothelial nitric oxide synthase in vascular disease: from marvel to menace. Circulation 113:1708–1714
33. **Sanada S, Kitakaze M, Node K, Takashima S, Ogai A, Asanuma H, Sakata Y, Asakura M, Ogita H, Liao Y, Fukushima T, Yamada J, Minamino T, Kuzuya T, Hori M** 2001 Differential subcellular actions of ACE inhibitors and AT(1) receptor antagonists on cardiac remodeling induced by chronic inhibition of NO synthesis in rats. Hypertension 38:404–411
34. **Kalra D, Sivasubramanian N, Mann DL** 2002 Angiotensin II induces tumor necrosis factor biosynthesis in the adult mammalian heart through a protein kinase C-dependent pathway. Circulation 105: 2198–2205
35. **Chintalgattu V, Katwa LC** 2004 Role of protein kinase CΔ in endothelin-induced type I collagen expression in cardiac myofibroblasts isolated from the site of myocardial infarction. J Pharmacol Exp Ther 311:691–699
36. **Zhang GX, Nagai Y, Nakagawa T, Miyanaka H, Fujisawa Y, Nishiyama A, Izuishi K, Ohmori K, Kimura S** 2007 Involvement of endogenous nitric oxide in angiotensin II-induced activation of vascular mitogen-activated protein kinases. Am J Physiol Heart Circ Physiol 293:H2403–H2408
37. **Vivar R, Soto C, Copaja M, Mateluna F, Aranguiz P, Muñoz JP, Chiong M, Garcia L, Letelier A, Thomas WG, Lavandero S, Diaz-Araya G** 2008 Phospholipase C/protein kinase C pathway mediates angiotensin II-dependent apoptosis in neonatal rat cardiac fibroblasts expressing AT1 receptor. J Cardiovasc Pharmacol 52: 184–190
38. **Olson ER, Shamhart PE, Naugle JE, Meszaros JG** 2008 Angiotensin II-induced extracellular signal-regulated kinase 1/2 activation is mediated by protein kinase CΔ and intracellular calcium in adult rat cardiac fibroblasts. Hypertension 51:704–711
39. **Li S, Galbiati F, Volonte D, Sargiacomo M, Engelman JA, Das K, Scherer PE, Lisanti MP** 1998 Mutational analysis of caveolin-induced vesicle formation. Expression of caveolin-1 recruits caveolin-2 to caveolae membranes. FEBS Lett 434:127–134
40. **Wunderlich C, Schober K, Kasper M, Heerwagen C, Marquetant R, Ebner B, Forkmann M, Schoen S, Braun-Dullaeus RC, Schmeisser A, Strasser RH** 2008 Nitric oxide synthases are crucially involved in the development of the severe cardiomyopathy of caveolin-1 knockout mice. Biochem Biophys Res Commun 377:769–774
41. **Shah AM, MacCarthy PA** 2000 Paracrine and autocrine effects of nitric oxide on myocardial function. Pharmacol Ther 86:49–86
42. **Yamashita T, Yamamoto E, Kataoka K, Nakamura T, Matsuba S, Tokutomi Y, Dong YF, Ichijo H, Ogawa H, Kim-Mitsuyama S** 2007 Apoptosis signal-regulating kinase-1 is involved in vascular endothelial and cardiac remodeling caused by nitric oxide deficiency. Hypertension 50:519–524
43. **Paradis P, Dali-Youcef N, Paradis FW, Thibault G, Nemer M** 2000 Overexpression of angiotensin II type I receptor in cardiomyocytes induces cardiac hypertrophy and remodeling. Proc Natl Acad Sci USA 97:931–936
44. **Song KS, Scherer PE, Tang Z, Okamoto T, Li S, Chafel M, Chu C, Kohtz DS, Lisanti MP** 1996 Expression of caveolin-3 in skeletal, cardiac, and smooth muscle cells. Caveolin-3 is a component of the sarcolemma and co-fractionates with dystrophin and dystrophin-associated glycoproteins. J Biol Chem 271:15160–15165
45. **Schlegel A, Wang C, Pestell RG, Lisanti MP** 2001 Ligand-independent activation of oestrogen receptor α by caveolin-1. Biochem J 359:203–210
46. **Lu ML, Schneider MC, Zheng Y, Zhang X, Richie JP** 2001 Caveolin-1 interacts with androgen receptor. A positive modulator of androgen receptor mediated transactivation. J Biol Chem 276:13442–13451
47. **Kim HP, Lee JY, Jeong JK, Bae SW, Lee HK, Jo I** 1999 Nongenomic stimulation of nitric oxide release by estrogen is mediated by estrogen receptor α localized in caveolae. Biochem Biophys Res Commun 263:257–262
48. **Grossmann C, Freudinger R, Mildenberger S, Husse B, Gekle M** 2008 EF domains are sufficient for nongenomic mineralocorticoid receptor actions. J Biol Chem 283:7109–7116
49. **Hill WG, An B, Johnson JP** 2002 Endogenously expressed epithelial sodium channel is present in lipid rafts in A6 cells. J Biol Chem 277:33541–33544

Downloaded from https://academic.oup.com/endo/article/151/3/1236/2456616 by guest on 10 April 2024